Supporting Information

Choppara et al. 10.1073/pnas.1705954115

SI Materials and Methods

Cell Culture, Synchronization, and Drug Treatments. HEK293T and MCF7 cells were obtained from the American Type Culture Collection and cultured in DMEM supplemented with 10% FBS (Sigma). HEK293T cells were synchronized at G1/S using hydroxyurea (1.5 mM) for 20 h or at G2/M using nocodazole (100 ng/mL) for 16 h and then released from synchronization by removing the drug-containing media, washing twice with DMEM, and growing in complete media. To evaluate cell-cycle distribution, synchronized cells collected at the indicated time points were fixed in 95% ethanol for 24 h at 4 °C. The fixed cells were washed twice with PBS and incubated with 50 μg/mL propidium iodide and 50 μg/mL RNase-A (Sigma) in PBS supplemented with 2 mM $MgCl_2$ for 30 min at 37 °C. After being washed, cells were suspended in PBS for further analysis. Data were acquired using a FACS Calibur flow cytometer (BD Biosciences) and analyzed using FlowJo v.10.0.7.

For AKT inhibition, cells were treated with 5 μM of an AKT inhibitor (Calbiochem; catalog no. 124005) for 24 h. For experiments involving DNA damage, cells were irradiated with 10 Gy for 4 h using a Co^{60} irradiation chamber or treated with 10 μM doxorubicin or etoposide (Sigma) for 24 h.

Plasmids, Mutagenesis, and RNAi-Mediated Knockdown. The plasmid expressing myc-FBXO31 has been previously described (5). Plasmids expressing HA-CDH1 (plasmid #11596) and HA-CDC20 (plasmid #11594) were obtained from Addgene. Plasmids expressing full-length wild-type FBXO31, the FBXO31(ΔD1) deletion mutant, and FBXO31(1-100) were generated by subcloning an FBXO31 PCR product (see Table S1 for primer sequences) in-frame into p3xFLAG-Myc-CMV (Sigma). The FBXO31 mutants FBXO31(R64A/L67A) and FBXO31(S33A) were generated using a site-directed mutagenesis kit (Stratagene) (see Table S1 for primer sequences). The constructs were transiently transfected into cells using Lipofectamine-2000 (Invitrogen). The plasmid expressing GST-FBXO31 was generated by subcloning an FBXO31 PCR product in-frame into pGEX-4T3 (GE Healthcare Life Sciences); the GST-FBXO31(S33A) derivative was generated by site-directed mutagenesis.

For generating knockdown cell lines, cells were stably transduced in the presence of polybrene (10 μg/mL) with the following shRNA lentiviruses from Open Biosystems/GE Dharmacon: APC2 (V3LHS_303044, V2LHS_303046), APC11 (V3LHS_365037, V3LHS_365038), CDH1 (V3LHS_334516, V2LHS_115164), CDC20 (V3LHS_363298, V2LHS_112883), AKT (V2LHS_188525, V2LHS_287019), ATM (V2LHS_192880, V2LHS_348), or DNA-PKcs/PRKDC (TRCN0000006259). Transduced cells were then selected with puromycin (2 μg/mL) for 7 d.

qRT-PCR. Total RNA was isolated using TRIzol (Invitrogen), and reverse transcription was performed followed by quantitative real-time PCR with SYBR Green supermix (TAKARA) using primers for *FBXO31* (forward, 5′-GATCCACCTGATGGAGAGGA-3′; reverse, 5′-TGCACTTGGTGGAGAACTCA-3′) and *GAPDH* (forward, 5′-CAATGACCCCTTCATTGACC-3′; reverse, 5′-GACAAGCTTCCCGTTCTCAG-3′), which was used as the normalizing control.

Immunoblotting and Coimmunoprecipitation. Protein extracts were prepared, and immunoblotting and coimmunoprecipitation were performed as described previously (11) using the following antibodies: AKT (Cell Signaling Technology, 9272S), phospho-AKT (Ser473) (Cell Signaling Technology, 4058S), ATM (Santa Cruz, sc-53173), phospho-ATM pS1981 (Rockland, 200–301-400), APC2 (Santa Cruz, sc-20984), APC11 (Santa Cruz, sc-20990), CDC20 (Santa Cruz, sc-7358), CDH1 (Sigma, C-7885), cyclin A (Santa Cruz, sc-751), cyclin B (Santa Cruz, sc-594), DNAPKcs (Abcam, ab70250), DNA PKcs (phospho S2056) (Abcam, ab124918), FBXO31 (Sigma, F4431), SKP2 (Santa Cruz, sc-7164), phospho-Ser (Cell Signaling Technology, 9606S), phospho-Thr (Cell Signaling Technology, 9391S), α-tubulin (Sigma, T5168), β-actin (Sigma, A2228), FLAG (Sigma, F1804), HA (Santa Cruz, sc-7392), c-myc (Roche, 11667149001), His (Thermo Scientific, MA1-21315), and, as a control, rabbit IgG (Sigma, I5006) or mouse IgG (Sigma, I5381) isotype controls. For the experiment in Fig. S9*C*, cells were treated with 10 μM of the ATM inhibitor KU-55933 (Tocris Biosciences) for 12 h. For all coimmunoprecipitation assays, cells were pretreated with 5 μM MG132 (Sigma) for 8 h before the preparation of protein extracts and immunoprecipitated with respective antibodies overnight at 4 °C followed by incubation with protein-G agarose beads. Eluted immuno-complexes were subjected to immunoblotting with respective antibodies.

Cycloheximide Chase. For the experiments monitoring stability of FBXO31, HEK293T or MCF7 cells were transfected with HA-CDH1 or HA-CDC20, and 36-h posttransfection cells were treated with 40 μg/mL cycloheximide (Sigma) for 0, 1, 2, 4 and 8 h. Stable knockdown cell lines expressing NS, CDH1, or CDC20 shRNAs were treated with cycloheximide as described above. Total cell extracts were subjected to immunoblotting with anti-FBXO31, anti-HA, and anti-tubulin antibodies. Band intensities were quantified using Image J software version 1.47v (NIH), and the ratio of the relative levels of FBXO31 and α-tubulin or β-actin at each time point time 0 was set to 100%.

In Vitro Kinase Assays. In vitro kinase assays were performed as described previously (11). Briefly, 293T cells were transfected with a plasmid expressing Flag-tagged AKT (Addgene plasmid #1477). Cell lysates were prepared by resuspension in modified TGN buffer [50 mM Tris at pH 7.5, 150 mM NaCl, 1% Tween 20, 0.3% Nonidet P-40, 1 mM sodium fluoride, 1 mM Na_3VO_4, 1 mM phenylmethylsulfonyl fluoride, and a protease inhibitor mixture (Roche)]. Cell lysates were incubated with an anti-Flag M2 antibody (Sigma) and protein A/G-agarose over night at 4 °C. The precipitated beads were washed with TGN buffer followed by TGN buffer plus 0.5 M LiCl and two washes with kinase buffer (50 mM Tris, pH 7.5, 20 mM $MgCl_2$, 1 mM EGTA, 2 mM DTT, 0.1 mM $NaVO_4$, 0.03% Brij-35). Finally, the pellet was resuspended in a 50-μL kinase buffer containing 10 μCi [γ-^{32}P]ATP and 5 μg GST-FBXO31 or GST-FBXO31(S33A). The kinase reaction was incubated for 20 min at 30 °C and stopped by the addition of SDS/PAGE protein sample buffer. Proteins were separated by SDS/PAGE, transferred to nitrocellulose, and visualized by autoradiography.

Ubiquitination Assays. For the in vivo ubiquitination assay, HEK293T cells were cotransfected with plasmids expressing His-tagged ubiquitin (Addgene plasmid #18712), HA-CDH1 or HA-CDC20, and Flag-FBXO31(WT), Flag-FBXO31(ΔD1), Flag-FBXO31(R64A/L67A), or Flag-FBXO31(S33A). Cells were pretreated with MG132, 5 h before extract preparation. Ubiquitylated proteins were purified under stringent denaturing conditions using Ni-NTA beads and immunoblotted using an anti-Flag antibody. For the assay shown in Fig. S7*A*, cells were treated with 5 μM AKT Inhibitor for 24 h, and protein extracts were

immunoprecipitated with anti-FBXO31 antibody and immunoblotted using the K48-Ub antibody (Cell Signaling Technology, 8081S).

The in vitro ubiquitination assay was performed as described previously (10). Briefly, HEK293T cells were transfected with plasmids expressing HA-CDH1 or HA-CDC20. CDH1- or CDC20-containing APC/C complexes were immunopurified and mixed with bacterially purified recombinant GST-FBXO31, 0.1 μM UBE1, 0.25 μM UBCH3, 0.25 μM UBCH5C, 1 μM ubiquitin aldehyde, 2 μg/μL ubiquitin, and 1× magnesium/ATP mixture (all from Boston Biochem) in the presence or absence of immunopurified Flag-AKT (expressed in HEK293T cells using Addgene plasmid #1477). Reaction mixtures were incubated for 2 h at 30 °C and then analyzed by immunoblotting. For quantification presented in Figs. S6 *A* and *B* and S7*B*, the intensity of the ubiquitin signal (the entire smear) was measured using Image J software version 1.47v (NIH), and the background level of ubiquitination (in the assay reaction containing His-Ub, lane 1) was subtracted. The results were then normalized to that obtained in assay reactions containing His-Ub and either HA-CDH1 or HA-CDC20, which was set to 1. For the quantification in Fig. S7*A*, the intensity of the ubiquitin signal was measured, and the K48-Ub signal in the reaction in the absence of AKT-I was set to 100%.

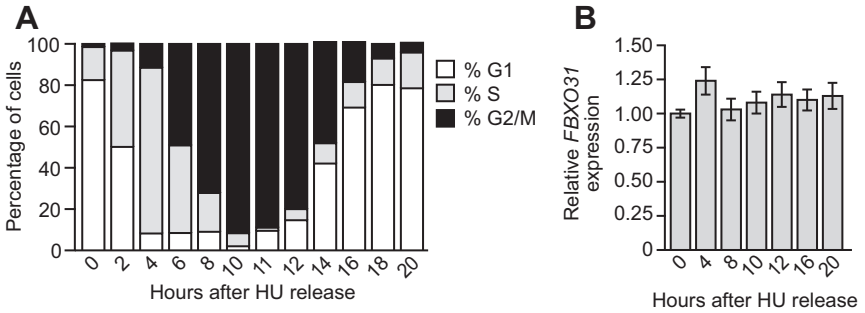

Fig. S1. FACS and qRT-PCR analyses related to Fig. 1*A*. (*A*) Bar graph of FACS analysis showing the distribution of cells in each phase of the cell cycle at each time point following release from HU synchronization. (*B*) qRT-PCR analysis monitoring *FBXO31* mRNA levels in HEK293T cells following HU synchronization and release. Data are represented as mean ± SD.

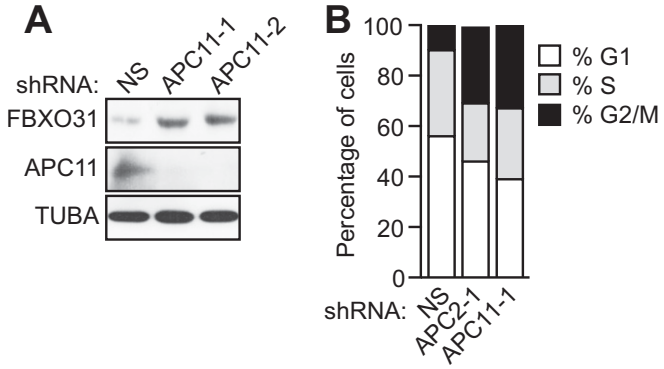

Fig. S2. Knockdown of APC11 results in increased FBXO31 protein levels, and knockdown of APC2 or APC11 results in an altered cell-cycle profile. (*A*) Immunoblot analysis monitoring the levels of FBXO31 in HEK293T cells expressing a NS shRNA or one of two unrelated APC11 shRNAs. α-Tubulin (TUBA) was monitored as loading control. (*B*) Bar graph of FACS analysis showing the distribution of cells in each phase of the cell cycle in HEK293T cells expressing a NS, APC2, or APC11 shRNA. The results show that knockdown of APC2 or APC11 results in a small increase in cells in G2/M. FBXO31 levels are high in early G2 through G2/M (Fig. 1*A*), in which APC/C is known to be inactive. Therefore, the increase in the percentage of cells in G2/M that occurs following knockdown of APC2 or APC11 likely contributes to the increased FBXO31 levels that we observe in these cells (*A* and Fig. 1*B*).

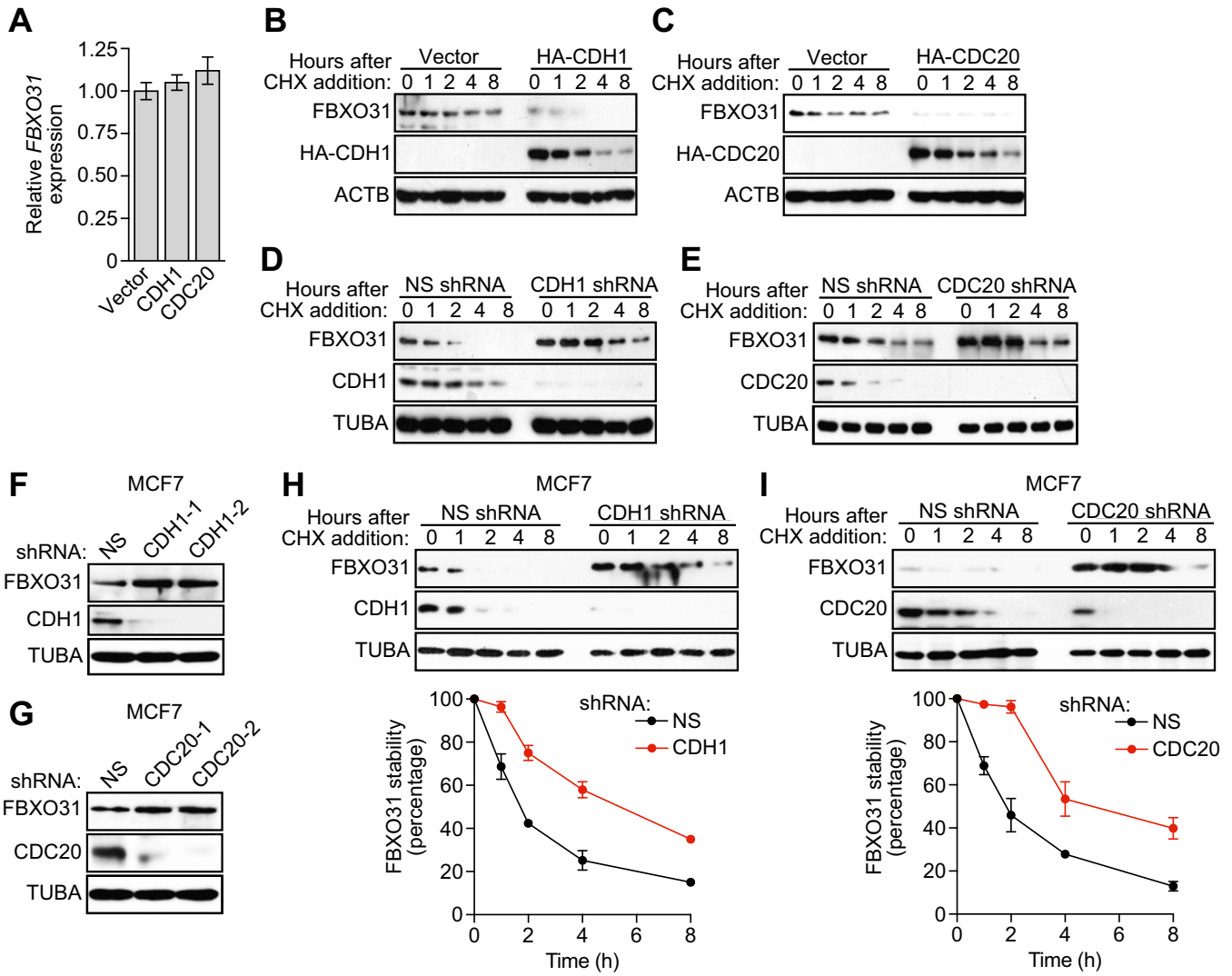

Fig. S3. FBXO31 protein levels are regulated by CDH1 and CDC20. (*A*) qRT-PCR analysis monitoring expression of *FBXO31* in HEK293T cells expressing vector, HA-CDH1, or HA-CDC20. The results were normalized to that obtained with the vector control, which was set to 1. (*B* and *C*) Cycloheximide chase/immunoblot assay monitoring FBXO31 stability in HEK293T cells expressing vector, HA-CDH1 (*B*), or HA-CDC20 (*C*). The immunoblots correspond to the graphs shown in Fig. 1 *F* and *G*. (*D* and *E*) Cycloheximide chase/immunoblot assay monitoring FBXO31 stability in HEK293T cells expressing a NS shRNA, CDH1 shRNA (*D*), or CDC20 shRNA (*E*). These immunoblots correspond to the graphs shown in Fig. 1 *J* and *K*. (*F* and *G*) Immunoblot analysis monitoring the levels of FBXO31 in MCF7 cells expressing a NS shRNA or one of two unrelated CDH1 (*F*) or CDC20 (*G*) shRNAs. (*H* and *I*) Cycloheximide chase/immunoblot assay monitoring FBXO31 stability in MCF7 cells expressing a NS shRNA, CDH1 shRNA (*H*), or CDC20 shRNA (*I*). Data are represented as mean ± SD.

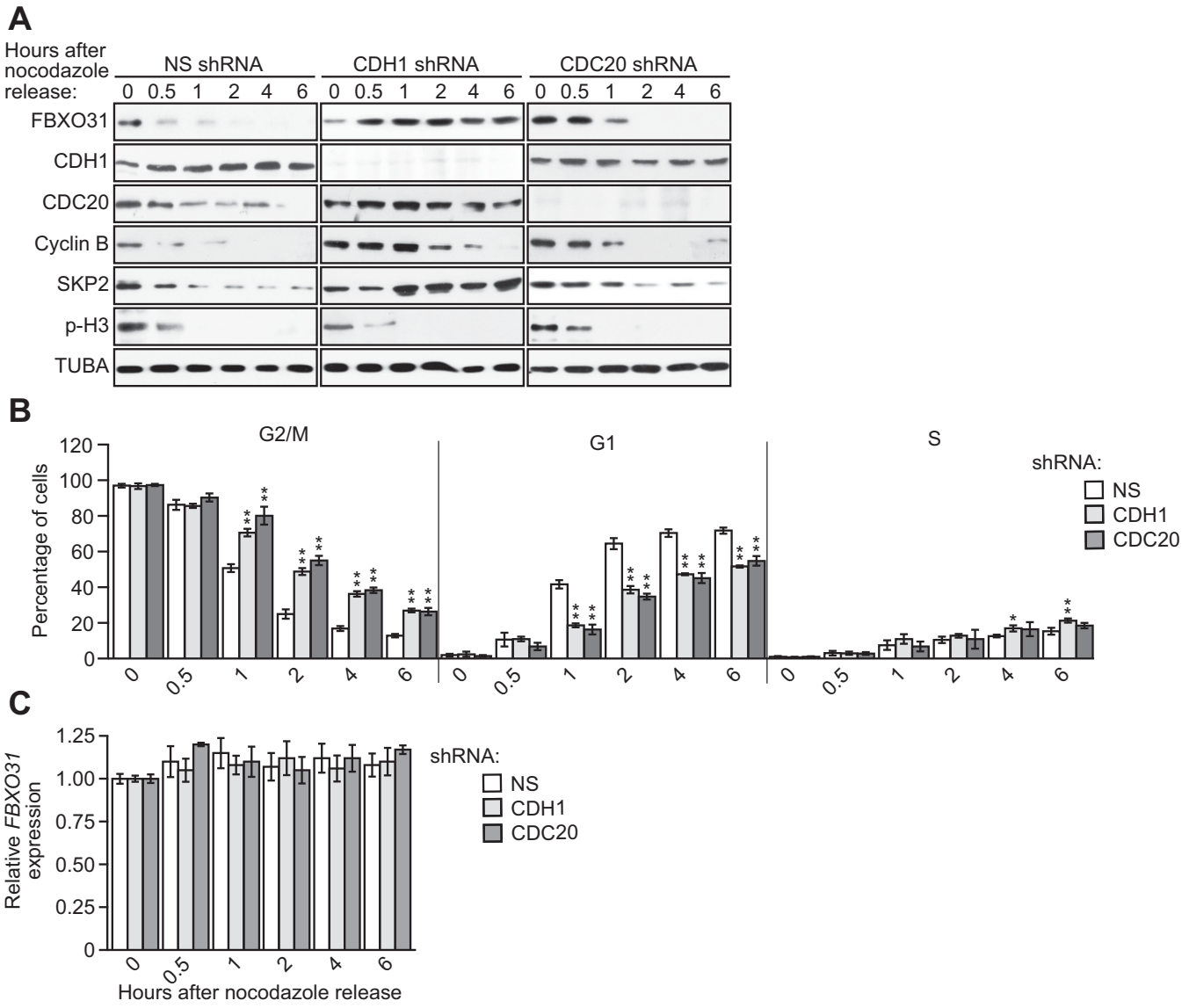

Fig. S4. CDH1 and CDC20 promote degradation of FBXO31 during the G1 and late M phases of the cell cycle, respectively. (*A*) Immunoblot monitoring FBXO31, cyclin B, CDH1, CDC20, SKP2, and phospho-histone H3 (p-H3) in HEK-293T cells synchronized by nocodazole following release after indicated time points. (*B*) Bar graph of FACS analyses showing the distribution of cells in each phase of the cell cycle at each time point. The *t* tests were performed in GraphPad Prism using the original false discovery rate method of Benjamini and Hochberg, with $Q = 1\%$ (36). The results demonstrate that there is a statistical difference in the cell-cycle profiles in cells expressing a CDH1 or CDC20 shRNA relative to cells expressing a NS shRNA. Data are represented as mean ± SD ($n = 3$ biological replicates). $*P < 0.05$, $**P < 0.01$. The results show that knockdown of CDH1 or CDC20 results in a small increase in cells in G2/M. FBXO31 levels are high in early G2 through G2/M (Fig. 1*A*), in which APC/C is known to be inactive. Therefore, the increase in the percentage of cells in G2/M that occurs following knockdown of CDH1 or CDC20 likely contributes to the increased FBXO31 levels that we observe in these cells (Fig. 1 *H* and *I*). (*C*) qRT-PCR analysis monitoring *FBXO31* mRNA levels in HEK293T cells following nocodazole synchronization and release. Data are represented as mean ± SEM.

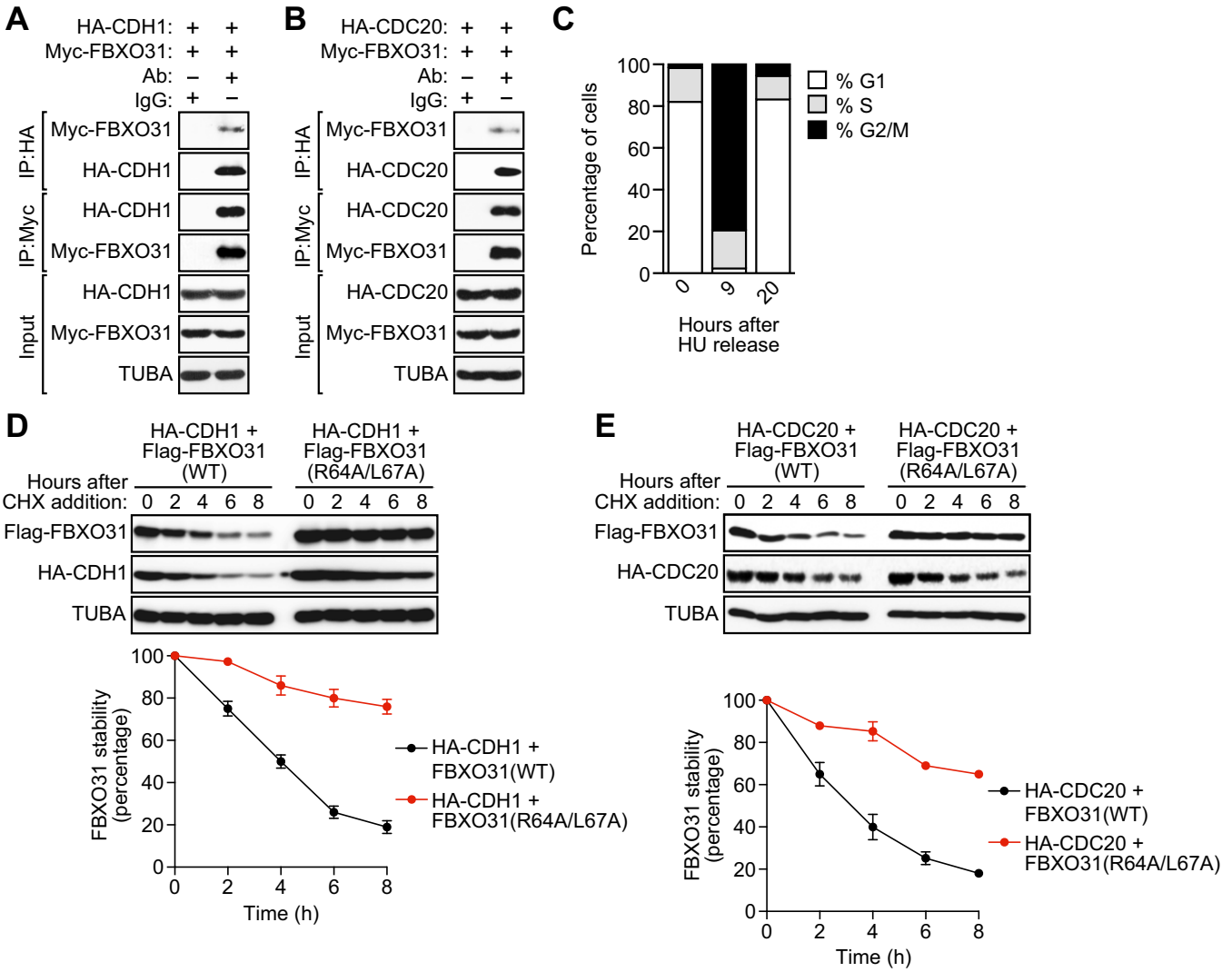

Fig. S5. Additional experiments related to Fig. 2. (*A* and *B*) Coimmunoprecipitation analysis monitoring the interaction between ectopically expressed myc-FBXO31 and HA-CDH1 (*A*) or HA-CDC20 (*B*) in HEK293T cells. IgG was used as a nonspecific control. (*C*) Bar graph of FACS analysis showing the distribution of cells in each phase of the cell cycle at 0, 9, and 20 h following release from HU synchronization. (*D* and *E*, *Top*) Cycloheximide chase/immunoblot assay monitoring FBXO31 stability in HEK293T cells expressing Flag-FBXO31(WT) or Flag-FBXO31(R64A/L67A) and HA-CDH1 (*D*) or HA-CDC20 (*E*). (*Bottom*) Quantification of immunoblots. Data are represented as mean ± SD.

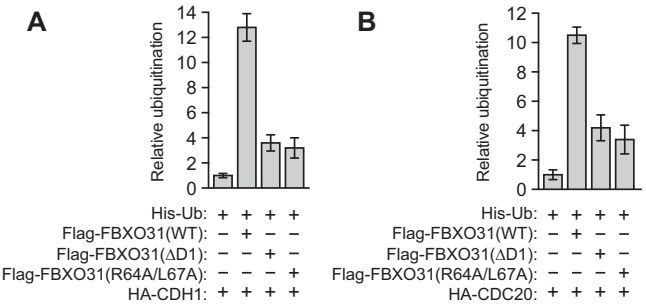

Fig. S6. Quantification of the in vivo ubiquitination assays of Fig. 3 *A* and *B*. Quantification of the intensity of the ubiquitin signal in the in vivo ubiquitination assays shown in Fig. 3*A* (*A*) and Fig. 3*B* (*B*). The data presented here correspond to lanes 2, 4, 6, and 8 of Fig. 3 *A* and *B*. The ubiquitin signal is normalized relative to that obtained in control reactions containing His-Ub and either HA-CDH1 (*A*) or HA-CDC20 (*B*), which was set to 1. Data are represented as mean ± SD.

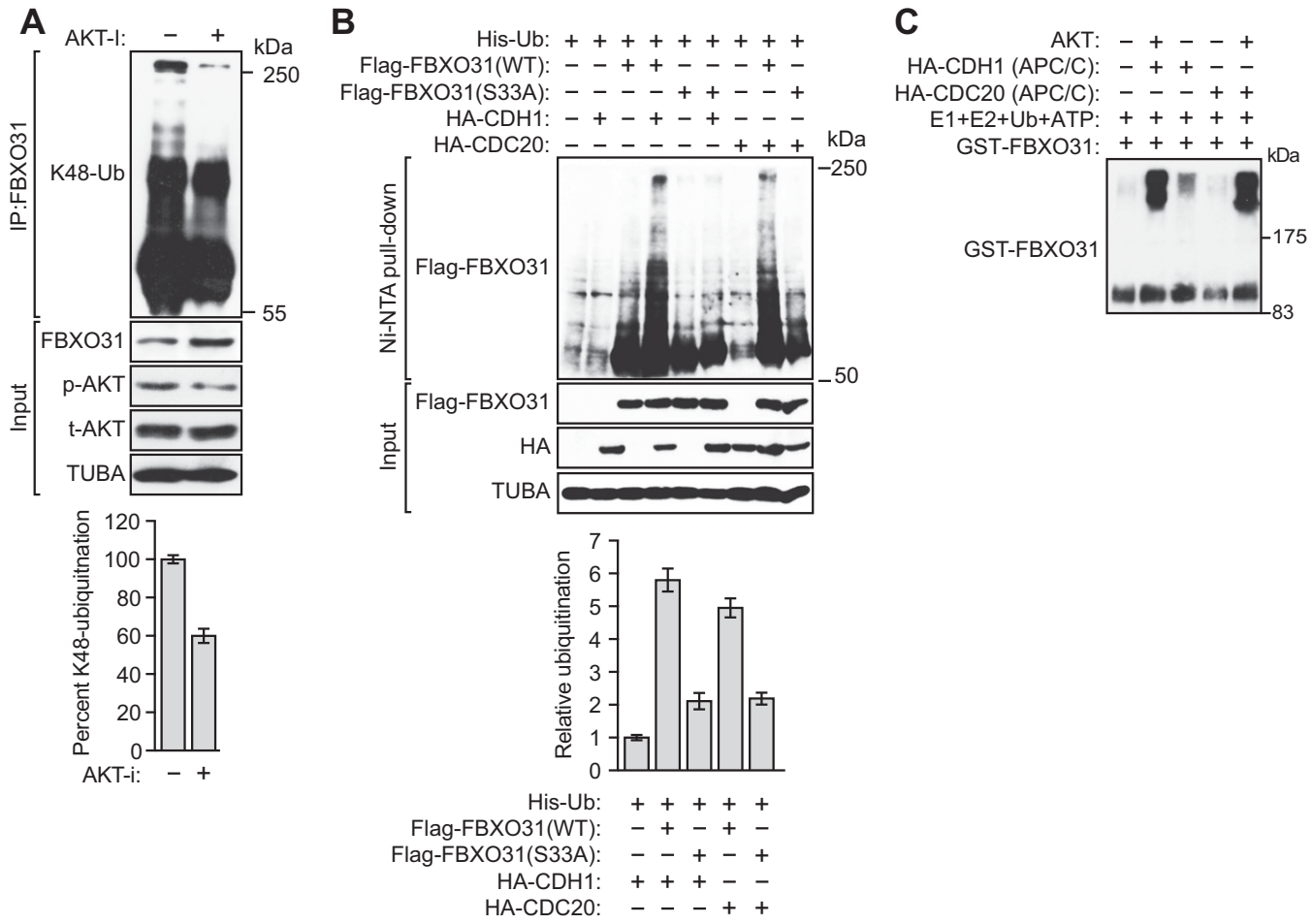

Fig. S7. Additional experiments related to Fig. 3. (*A*, *Top*) In vivo ubiquitination assay monitoring ubiquitination of endogenous FBXO31 as determined using a K48-linked ubiquitin antibody in the presence or the absence of AKT inhibitor (AKT-I). (*Bottom*) Quantification of the percent K48 ubiquitination. (*B*, *Top*) In vivo ubiquitination assay. HEK293T cells were cotransfected with plasmids expressing His-ubiquitin, Flag-FBXO31(WT), Flag-FBXO31(S33A), and HA-CDH1 or HA-CDC20. Proteins bound to His-ubiquitin were purified by Ni-NTA pull-down, washed, and eluted in imidazole. Ubiquitinated Flag-FBXO31 was detected using an anti-Flag antibody. (*Bottom*) Quantification. (*C*) In vitro ubiquitination assay monitoring the ability of a purified APC/C-CDC20 or APC/C-CDH1 to ubiquitinate GST-FBXO31 in the presence or the absence of AKT. Data are represented as mean ± SD.

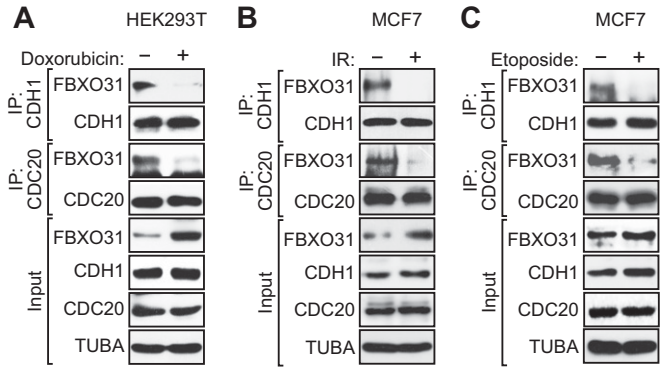

Fig. S8. Additional experiments confirming that the interaction between FBXO31 and CDH1 or CDC20 is perturbed following DNA damage. (*A*) Coimmunoprecipitation monitoring the interaction between endogenous FBXO31 and CDH1 or CDC20 in unsynchronized HEK293T cells treated in the presence or the absence of doxorubicin. (*B* and *C*) Coimmunoprecipitation monitoring the interaction between endogenous FBXO31 and CDH1 or CDC20 in unsynchronized MCF7 cells treated in the presence or the absence of IR (*B*) or etoposide (*C*).

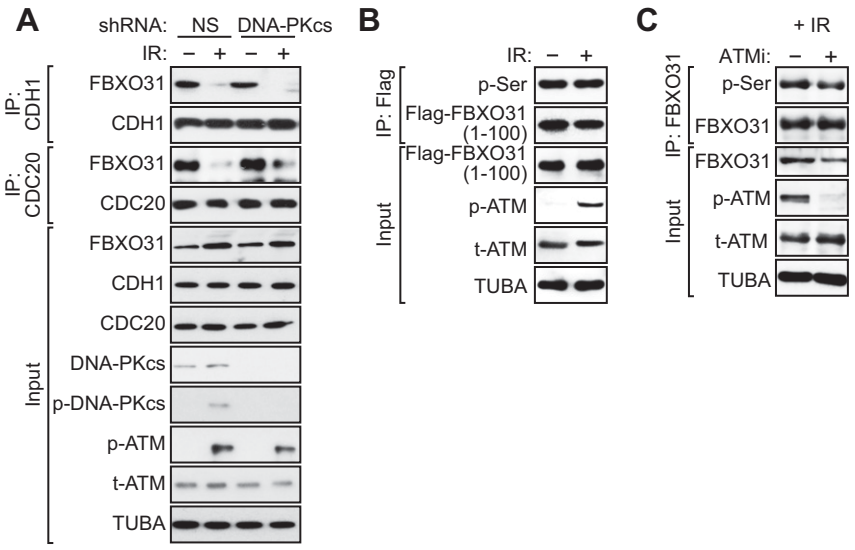

Fig. S9. Additional experiments related to Fig. 4. (*A*) Coimmunoprecipitation monitoring the interaction between endogenous FBXO31 and CDH1 or CDC20 in HEK293T cells expressing a NS or DNA-PKcs shRNA, with or without IR. The results show that, unlike in ATM-depleted cells (Fig. 4*B*), knockdown of DNA-PKcs does not stabilize the interaction of FBXO31 with CDC1 or CDC20. These results strengthen our conclusion that loss of interaction of FBXO31 with CDH1 and CDC20 following DNA damage is a direct consequence of ATM phosphorylation rather than an indirect effect of activation of the DNA damage response. (*B*) Coimmunoprecipitation monitoring the presence of phosphorylated Ser (p-Ser) in the Flag immunoprecipitate from HEK293T cells expressing a Flag-tagged N-terminal fragment of FBXO31, amino acids 1–100 [FBXO31(1–100)], which contains the AKT phosphorylation site but not the ATM phosphorylation site. The results show that the FBXO31(1–100) derivative was phosphorylated in unstressed, untreated cells, as expected, and that the phosphorylation status did not change following treatment with IR. These results suggest that AKT-mediated phosphorylation of Ser-33 is not reduced following DNA damage. (*C*) Coimmunoprecipitation monitoring the presence of p-Ser in the FBXO31 immunoprecipitate from HEK293T cells treated with IR in the presence or the absence of an ATM inhibitor (ATMi). The results show that FBXO31 serine phosphorylation does not increase upon treatment with ATMi, indicating that ATM-mediated phosphorylation of FBXO31 does not impede its phosphorylation by AKT.

Table S1. Primer sequences used for generating various FBXO31 constructs

Constructs	Primers (5′-3′)
Flag-FBXO31	Forward-AAGCTTATGGCGGTGTGTGCTCGC
	Reverse-GAATTCTCAGGAGGTGAGGGACTG
Flag-FBXO31(ΔD1)	Forward-AAGCTTCCCGAGCTGCTGGTGGAGATC
	Reverse-GAATTCTCAGGAGGTGAGGGACTG
Flag-FBXO31(1–100)	Forward-AAGCTTATGGCGGTGTGTGCTCGC
	Reverse-GAATTCGCCTCCTCACGGCAACGCCT
Flag-FBXO31(R64A/L67A)	Forward-CGCCGCCGCCCCCGGCCTGCTCGGCGCTGGAGCTGCCGCCC
	Reverse-GGGCGGCAGCTCCAGCGCCGAGCAGGCCGGGGGCGGCGGCG
Flag-FBXO31(S33A)	Forward-GGCGGCCGACGCCGAGCCGGACACAGAC
	Reverse-GCCGTCTCGGCCGGGCCC